The Origin of Electrochemical Promotion in Heterogeneous Catalysis: Photoelectron Spectroscopy of Solid State Electrochemical Cells

ARTICLE *in* THE JOURNAL OF PHYSICAL CHEMISTRY B · DECEMBER 1999

Impact Factor: 3.3 · DOI: 10.1021/jp993037i

4 AUTHORS, INCLUDING:

Federico J. Williams
University of Buenos Aires
87 PUBLICATIONS **1,402** CITATIONS

SEE PROFILE

Richard Michael Lambert
University of Cambridge
194 PUBLICATIONS **6,727** CITATIONS

SEE PROFILE

The Origin of Electrochemical Promotion in Heterogeneous Catalysis: Photoelectron Spectroscopy of Solid State Electrochemical Cells

Federico J. Williams, Alejandra Palermo, Mintcho S. Tikhov, and Richard M. Lambert*

Department of Chemistry, University of Cambridge, Cambridge CB2 1EW, U.K.

Received: August 25, 1999; In Final Form: November 10, 1999

Electropumping of Na from or to a Na-β'' alumina solid electrolyte contacted with a thin film porous copper electrode results in fully reversible transport of Na to or from the vacuum-exposed Cu surface. The extent of pumping is controlled by the potential of the catalyst film (V_{WR}), measured with respect to a reference electrode. The time constants of these spill over and reverse spill over processes are short compared with 1 min. Photoelectron microscopy suggests that the spatial distribution of Na is fairly uniform. Over an extended range of catalyst potential ($\Delta V_{WR} \sim 1$ V), both the Na coverage (ϑ_{Na}) and the Cu work function (ϕ) scale linearly with V_{WR}. This is the same regime over which the rate and nitrogen selectivity of the Cu-catalyzed CO+NO reactions are greatly increased. The maximum Na coverage achieved by electro-pumping is ~0.06 monolayer, commensurate with the corresponding catalytic response of the system. At sufficiently high positive values of V_{WR}, this quantity becomes uncoupled from $\Delta\phi$, ϑ_{Na}, and the catalytic behavior. The possible origin of this uncoupling effect is discussed and a consistent explanation offered for the phenomenon of electrochemical promotion.

1. Introduction

The performance of dispersed metal catalysts may often be improved by purposeful addition of small amounts of promoter species which modify the surface chemistry.[1,2] Practical supported metal catalysts are relatively complex materials whose structure and composition have been optimized by empirical means. Although these procedures are effective, they provide little insight into the underlying phenomena that determine performance: in particular, they rarely shed any light on the mechanism of promoter action. Alkali metal compounds are commonly employed as promoters of metal catalysts, a fact that has stimulated much research on alkali adsorption using single-crystal model systems investigated by the methods of surface science.[3] Most of these single-crystal studies are carried out under conditions of ultrahigh vacuum. Although in favorable cases such data[4] can be directly related to the behavior of practical catalysts working at atmospheric pressure,[5] in general the linkage between the two is more tenuous.

An interesting electrochemically induced promoter effect *electrochemical promotion* (EP) provides an alternative approach to an understanding of promoter action. EP was discovered more than a decade ago[6] by Vayenas and co-workers who subsequently developed the methodology and laid down the basis for interpreting the effect. The technique entails electrochemical pumping of ions from a solid electrolyte to the surface of a porous, catalytically active metal film with which it is in contact. The effects of EP on catalytic activity and selectivity are generally reversible, reflecting the reversibility of the electrode reaction involving the promoter species. It is important to appreciate from the outset that one is not dealing with conventional electrocatalysis, which is a strictly Faradaic process: one mole of charge transported through the electrolyte results in one mole of chemical reaction at the working electrode. Under EP conditions, the electrochemically induced catalytic rate changes are typically 10^3-10^5 times greater than the rate of supply of promoter species. That is, one mole of charge transported results in 10^3-10^5 turnovers. Thus EP is strongly non-Faradaic, which is why its discoverers called the effect *non-Faradaic electrochemical modification of catalytic activity*, NEMCA.

It is helpful to consider a specific example, e.g., the use of Na-β'' alumina (a Na^+ conductor), as the solid electrolyte. Under forward bias Na^+ ions are transported to the working electrode where they are discharged at the metal electrode/solid electrolyte/gas three phase boundary. The resulting species (Na) spill over onto the surface of the metal catalyst, strongly altering its electronic properties. This Na-induced change in surface electronic properties is manifested by concomitant changes in (i) catalyst work function ($\Delta\phi$), (ii) adsorption enthalpies of adsorbed species, and (iii) activation energies of reactions involving these species. In practice, the state of the catalyst surface is conveniently monitored by following the changes in catalyst potential measured with respect to a reference electrode (ΔV_{WR}). Experiment shows that $e\Delta V_{WR}$ is usually of the same order as $\Delta\phi$, although the two quantities are not always identical.

Distinguishing features of EP systems include the following: (i) they permit in situ control of catalyst performance under conditions of turnover, (ii) the polycrystalline metal film/oxidic solid electrolyte system provides a reasonable approximation to conventional dispersed metal/metal oxide catalysts, (iii) these systems can be operated at atmospheric pressure and above, and (iv) EP samples are amenable to study by electron spectroscopy and related methods of investigation.

As a consequence of (i)−(iv) one may use electrochemical promotion to (i) elucidate reaction mechanisms[7,8] by studying the response of activity and selectivity to controlled changes in promoter levels, and (ii) develop new conventional catalytic systems,[9−11] based on the insight provided by the corresponding EP analogues.

* Corresponding author. E-mail: RML1@CAM.AC.UK. Fax + 44 1223 336362.

10.1021/jp993037i CCC: $19.00
Published on Web 12/28/1999

There is another cogent reason for carrying out fundamental research on EP: namely, that we need to understand the phenomenon inasmuch detail as possible so that a quantitative theoretical framework can be established. This is the principal aim of the present paper. X-ray and ultraviolet photoelectron spectroscopies (XPS and UPS) have been used to study the phenomena that underlie the EP effect. Specifically, we have investigated the electropumping and spillover of Na at the Na-β''alumina/copper interface where the electrode reaction is

$$Na^{+}_{(alumina)} + e^{-}_{(copper)} \leftrightarrow Na_{(copper)} \quad (1)$$

This system was chosen because the Cu-catalyzed NO+CO reaction exhibits large increases in both rate and selectivity toward nitrogen formation (as opposed to N_2O) when subjected to electrochemical promotion by Na.[12]

2. Experimental Methods

UPS and XPS measurements were performed under UHV conditions (base pressure $< 10^{-10}$ Torr) in a VG ADES 400 UHV spectrometer system. This was equipped for angle-resolved UPS/XPS with the sample under potentiostatic control, i.e., at elevated temperature and with potentials applied. XP spectra were acquired at a constant pass energy of 20 eV using an un-monochromated Mg Kα (1253.6 eV) source operated at 11 kV and 20 mA. Quoted binding energies are referred to the $Au4f_{7/2}$ emission at 83.8 eV from the Au wire that formed the electrical connection to the Cu working electrode. Work function changes were determined by measuring the change in secondary electron cutoff in the UP sepctrum relative to the Fermi edge. UP spectra were recorded using He I radiation (21.21 eV) and a constant pass energy of 2 eV. During acquisition of the UP spectra the analyzer was positioned at 7° with respect to the surface normal and the working electrode was biased −9.5 V with respect to ground. XP spectra were recorded the working electrode grounded and the analyzer at 35° with respect to the sample normal. The temperature chosen for these spectroscopic experiments was the same as that used in our investigation of the Cu-catalyzed CO+NO reaction under EP conditions.[12] It also lies in the regime where the ionic conductivity of the solid electrolyte is sufficiently high.

Synchrotron experiments were performed at the ESCA microscopy beamline on the ELETTRA light source, Trieste, Italy. The photon beam, provided by a spherical grating monochromator, was demagnified in the scanning photoemission microscope (SPEM) to a spot of 0.15 μm diameter using a zone plate optical system. Photoelectrons were collected with a 100-mm hemispherical analyzer mounted at 70° with respect to the sample normal and the incident photon beam. All experiments were performed with the working electrode grounded and at a photon energy of 490 eV. The SPEM operated in two modes: imaging and spectroscopic. Elemental mapping was performed by scanning the sample with respect to the focused beam with the analyzer tuned to the desired kinetic energy. In spectroscopic mode, core or valence spectra could be recorded from microspots on features selected from the elemental maps.

The solid-state electrochemical cells were prepared from a 1 cm × 1 cm × 1 mm wafers of polycrystalline Na-β'' alumina. Copper catalyst films (working electrode, W) were deposited by sputtering copper metal (thickness ~30 μm as estimated by SEM) on one face of each β'' alumina wafer. Gold counter (C) and reference (R) electrodes were similarly deposited on the opposite faces of the solid electrolyte wafers. (The reference is electrode is not a true reference electrode in the thermodynamic sense. For reasons discussed elsewhere[8] it should more correctly be termed a pseudoreference electrode.) The entire electrochemical cell was mounted on a sample holder made from a machinable ceramic and containing embedded electrically insulated Nichrome filaments that allowed resistively heating of the sample. This is illustrated in the upper part of Figure 1. All electrical connections were made of gold. Three samples were prepared and used to acquire the XPS, UPS, and synchrotron XPS data.

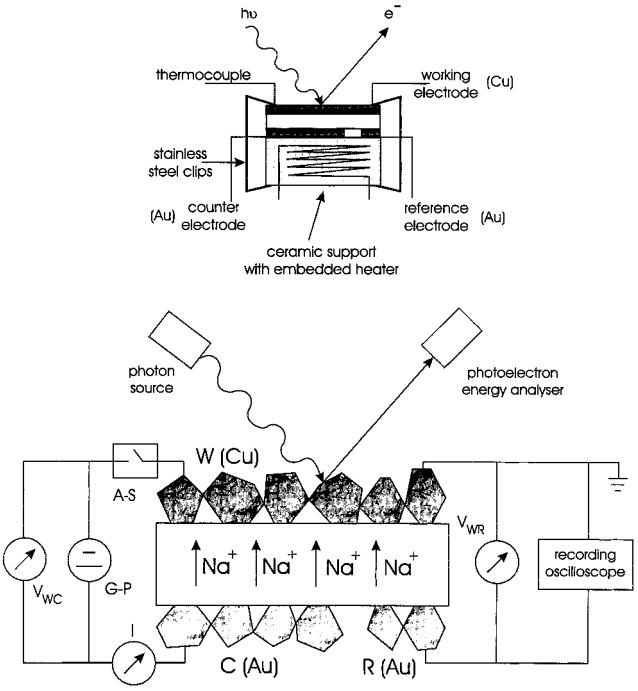

Figure 1. Sample holder and electrochemical cell (three electrode arrangement) used for the in situ XPS and UPS measurements.

A galvanostat−potentiostat (Ionic Systems) was used to maintain a potential difference (V_{WR}) between the working and reference electrodes (potentiostatic mode). In a separate control experiment, the ohmic drop free potential of the working electrode was determined using the current interruption technique.[13] Current interruption was achieved by means of an analogue switch (ADG201HS) with a response time of 50 ns. A digital oscilloscope was use to record the ohmic drop. The results showed that the ohmic drop contribution to V_{WR} could be neglected under all conditions. That is, the V_{WR} values reported below are true values. The lower part of Figure 1 shows the setup of the solid electrolyte electrochemical cell. It is configured as a three-electrode system, well-known in liquid-state electrochemistry.[14] Note that the experiments span a range of V_{WR} values of about 1 V. Larger excursions were not possible because they would necessitate application of large values V_{WC}, the voltage applied between the Cu working electrode and the Au counter electrode. These leads to electrolytic decomposition of the solid electrolyte accompanied by evolution of oxygen gas, detected mass spectrometrically.

3. Results and Discussion

3.1. XP Spectroscopy. Figure 2 shows Na 1s XP spectra obtained at 623 K as a function of catalyst potential (V_{WR}) under ultrahigh vacuum conditions. The +600 mV spectrum corresponds to the electrochemically cleaned sample; increasingly negative values of V_{WR} should correspond to increasing amounts of electropumped Na on the catalyst surface. Qualitatively, this is exactly what is observed, confirming that EP works by

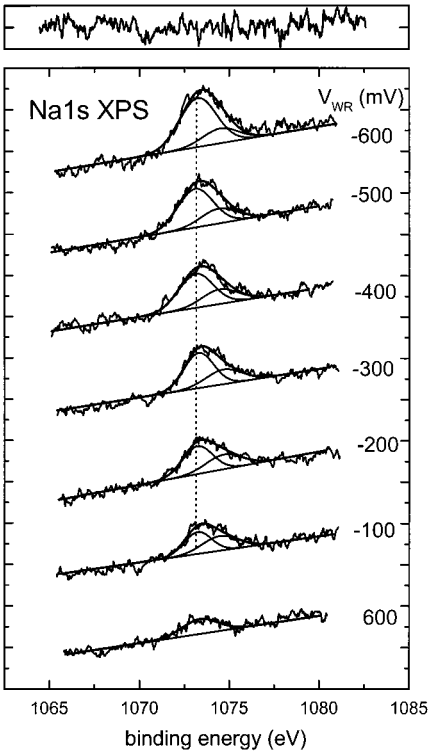

Figure 2. Na 1s XPS spectra showing the effect of catalyst potential on sodium coverage of the Cu film under UHV conditions at 623 K. Invariant component due to Na on Cu; shifting component due to Na in solid electrolyte.

supplying promoter species to the catalyst surface (the sampling depth in these experiments is ~1 nm). This spectral behavior was reversible and reproducible as a function of V_{WR}, in line with the reversible and reproducible catalytic response under reaction conditions at atmospheric.[12] Note that there is residual Na 1s emission from the electrochemically cleaned sample. To fully understand this, recall that the copper film is both thin and porous. The Na 1s emission envelope therefore comprises *two* components, one due to the Na present on the surface of the Cu film and the other due to Na in the β'' alumina electrolyte which is visible through the cracks and pores in the metal film. The component due to Na on the Cu catalyst exhibits invariant binding energy (BE) and increases in intensity with decreasing V_{WR}, as one would expect. The other component exhibits constant intensity and a systematic shift in *apparent* BE (ΔE_B). This shift is numerically equal to the change in V_{WR} (i.e., the change in catalyst overpotential), nicely confirming that the corresponding Na 1s emission arises from the solid electrolyte whose electrostatic potential differs from that of the Cu film by the amount ΔV_{WR}. A measure of the quality of the curve fitting procedure used in this analysis is provided by the residual that is displayed in the upper panel of Figure 2. The numerical correspondence between ΔV_{WR} and ΔE_B is made even more apparent by the results presented in Figure 3 which is based on a larger data set. The apparent binding energy shift of the Na component ascribed to the Na-β'' alumina has been plotted against ΔV_{WR}. These results confirm beyond doubt the interpretation offered above.

Figure 4 shows the integrated intensity of the Na 1s emission from the component associated with the Cu surface versus V_{WR}. Two points are very apparent. First, there is a region (~700 to ~300 mV) in which decreasing the catalyst potential does not pump XPS-detectable Na on the Cu surface. Second, for V_{WR} < ~300 mV, decreasing the catalyst potential causes a linear

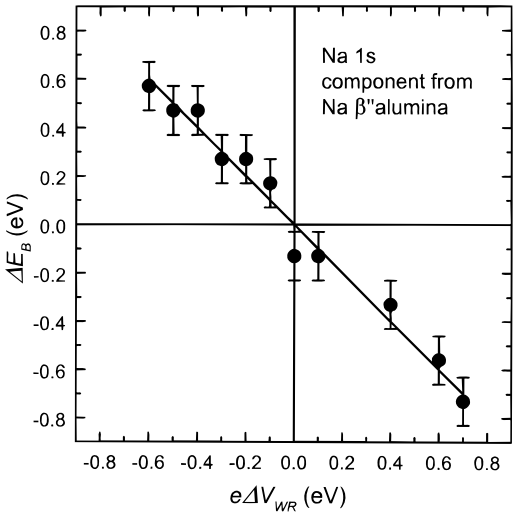

Figure 3. Binding energy shift of the Na 1s XPS component due to Na in the solid electrolyte as a function of the change in V_{WR}.

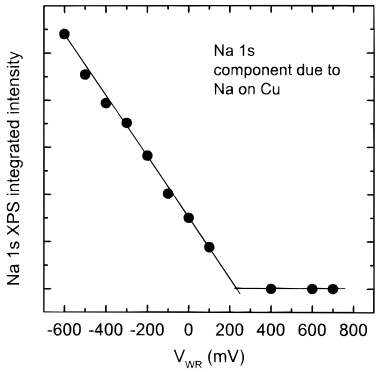

Figure 4. Integrated Na 1s XPS intensity from Na on Cu as a function of catalyst potential.

increase of the Na 1s XPS area. The first observation implies that at ~300 mV the Cu surface has been fully depleted of Na by electropumping. The second observation is equally interesting: once detectable Na is present on the Cu, the Na coverage changes linearly with V_{WR}. This is in excellent accord with the synchrotron data presented below.

Figure 5 shows synchrotron Na 2p XP spectra as a function of V_{WR} at $T = 523$ K. In this case it is evident that the component due to the Na present on the Na-β'' alumina is not detected. Only a single component is visible in the Na 2p emission. This exhibits invariant BE and grows in intensity as the catalyst potential is decreased (spectra 1−10). On the basis of the preceding arguments, we assign it to Na on the Cu surface. The reversibility of Na transport is made clear in Figure 5. Spectra were recorded in the time sequence 1−6 during which the Na coverage increased progressively as V_{WR} was altered from 400 to −700 mV. Switching to −400 mV (spectrum 7) decreased the amount of Na to a coverage intermediate between spectra 4 (−300 mV) and 5 (−500 mV). A further increase to +400 mV (spectrum 8) immediately cleaned the surface of Na; switching to −600 mV (spectrum 9) gave a coverage intermediate between spectra 5 and 6; switching to +600 mV again generated a clean surface (spectrum 10). That is, for a given value of V_{WR}, there was a specific amount of Na present on the Cu surface.

Unlike the laboratory XP spectra, the synchrotron measurement discriminates strongly against Na 2p photoelectrons from the underlying solid electrolyte. This is due to two factors, one relating to the incident photons, the other to the emitted

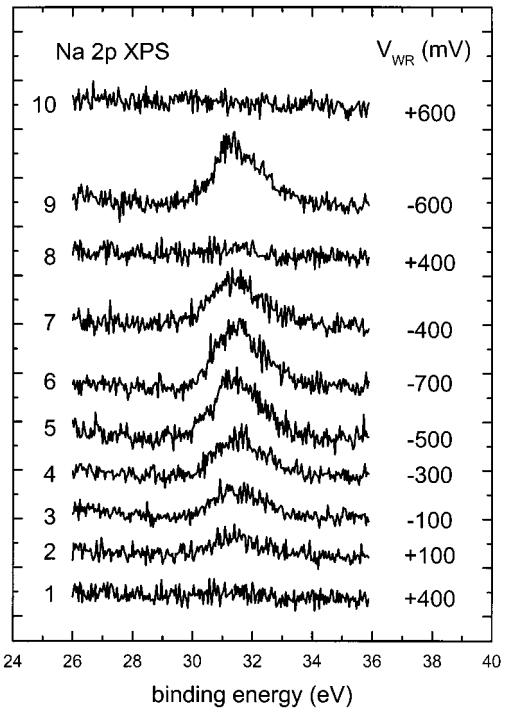

Figure 5. Synchrotron core level spectroscopy. Grazing electron exit Na 2p spectra as a function of V_{WR}. Cf. Figure 2; in this case only Na on Cu is detected.

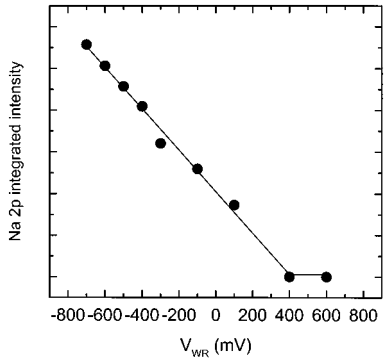

Figure 6. Integrated Na 2p intensity from Na on Cu as a function of V_{WR}.

electrons, as follows. (i) The X-ray beam diameter was only 0.15 μm, much smaller than the average Cu particle size (5 μm as estimated by SEM). Since the beam was adjusted so as to impinge on top of a Cu particle, the underlying electrolyte is effectively shielded from incident photons. (ii) The photoelectrons were detected at grazing exit angle (70° with respect to the sample normal) which enhances the surface sensitivity of the measurement.

Figure 6 shows the dependence of the integrated *raw* Na 2p emission intensity on catalyst potential. The behavior replicates that of the Na 1s intensity extracted for the invariant component in the spectra obtained with a laboratory source (Figure 4). Decreasing V_{WR} from ~700 to ~400 mV caused no increase in the Na 2p intensity. Further decrease in V_{WR} caused a linear increase in the Na coverage. This threshold behavior is also apparent in the $\Delta\phi$ data (see later) and in the catalytic response of the system.[12] It is discussed below.

In order to check whether the measured Na coverages corresponded to true steady-state values, we attempted to study the time dependence of the spillover process. Figure 7 shows a time sequence of Na 2p XP spectra obtained as V_{WR} was

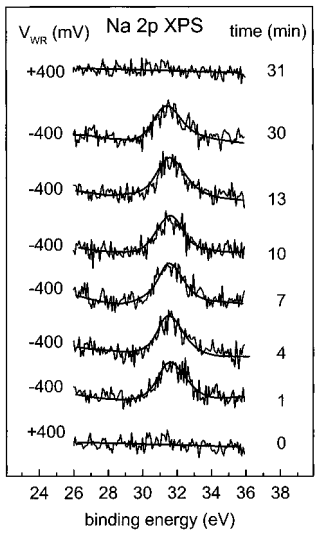

Figure 7. Synchrotron core level spectroscopy. Grazing electron exit Na 2p spectra as a function of time for different values of V_{WR}.

switched from +400 mV (electrochemically cleaned surface) to −400 mV (Na pumped to Cu surface) and back again to +400 mV (Na pumped away from Cu). The acquisition time per spectrum was ~1 min. It is apparent that the Na spillover and reverse spillover processes took place in less than one minute, after which the Na coverage remained constant with time. Therefore, we were not able to study the time dependence of the spillover process.

The spectroscopic data may be used to estimate Na surface coverages (ϑ_{Na}) using the relationship derived by Carley et al.[15]

$$\vartheta_{Na} = \frac{Y_m \sigma_s N \cos\psi \rho \lambda}{Y_s \sigma_m M_s} \quad (2)$$

Where Y_m is the integrated photoelectron signal from a particular subshell of the adatom (e.g., Na(1s)); Y_s is the integrated signal from the relevant subshell of the substrate (e.g., Cu2p)); σ_m and σ_s are the subshell photoionization cross sections for the adatom and substrate; M_s is the molecular weight of the substrate; ρ is the density of the substrate; λ is the escape depth in the substrate for the particular substrate subshell photoelectrons; ψ is the angle of detection with respect to the sample normal of the photoelectrons; and N is Avogadro's number.

On this basis, the data presented in Figure 4 yield a maximum Na concentration of 4.1×10^{14} atom/cm^2 for $V_{WR} = -600$ mV and the data presented in Figure 6 yield a maximum Na concentration of 3.4×10^{14} atm/cm^2 at $V_{WR} = -700$ mV. Thus the agreement between the calculated maximum sodium concentrations for two independent sets of data is good. If we assume a density of substrate atoms of 1.8×10^{15} atm/cm^2 (corresponding to Cu(111)), then the data in Figures 4 and 6 correspond to maximum sodium coverages of 0.22 and 0.18 monolayers, respectively. Note however that eq 2 is valid for an ideally flat substrate. Our samples are rough. Therefore eq 2 gives an overestimate of the sodium coverage, because the true metal surface area is greater than the geometrical area covered by Cu. A more precise estimate of the maximum achievable sodium coverage is provided by work function measurements, as discussed below.

3.3. Elemental Mapping by SPEM. By tuning the analyzer to the Cu 3d or Na 2p photoelectrons and scanning the sample, we obtained intensity maps which reflect the distribution of the elements at the surface with spatial resolution of 0.15 μm, as a

function of V_{WR} with the sample held at 523 K. Since we are dealing with rough surfaces (grain sizes ~5 μm) SPEM data are subject to topographical artifacts. We therefore treated the data using the algorithm recommended by Kiskinova et al.,[16,17] which is designed to normalize out intensity variations due to topographical features as opposed to true changes in elemental concentration. To our knowledge, these are the first measurements of their kind. We present them because they suggest that certain conclusions may be drawn tentatively. Clearly further developments along these lines would be desirable.

Figure 8 shows 25 μm × 25 μm typical Cu 3d and Na $2p_{3/2}$ intensity maps taken at 523 K for two V_{WR} values: +400 mV (Na-free surface) and −600mV (sodium coverage ~0.06 monolayers). The spectra in Figures 8c and d where taken from a microspot located at the center of each image. These spectra show that (i) at + 400 mV there is no detectable sodium at the point of analysis and (ii) at −600 mV there is sodium present at this point. Figure 8b and f show Cu 3d intensity maps for V_{WR} = + 400 mV and − 600 mV, respectively. The bright feature identifies a Cu-rich region, probably a large Cu crystallite, whereas the dark features could be due to cracks on the Cu surface or to shadowing of the Cu particles. These two images show that there was no thermal drift during the experiments—an important point when evaluating the significance of the Na maps. Figure 8a and e show the Na $2p_{3/2}$ maps corresponding to Figure 8b and f, respectively. Qualitatively, these images indicate that the amount of surface Na has been increased by electropumping. Additionally, the average spacing between the Na "spots" is small compared with the Cu crystallite size, suggesting that the spatial distribution of this Na is relatively uniform.

3.4. Work Function Changes. Work function measurements provide valuable complementary information about the surface processes occurring during spillover of electro-pumped Na. Figure 9 shows the work function changes of the copper film as a function of the ohmic-drop free potential V_{WR} at 623 K. The overall behavior mirrors that of the Na 1s and Na 2p Xp intensities (Figures 4 and 6). As with the XP intensities, the work function exhibits fully reversible dependence on V_{WR}. Two features are again noteworthy. First, there is a range of V_{WR} (400 mV to −100 mV) over which no changes in work function occur. Second, for $V_{WR} < -100$ mV, decreasing V_{WR} (i.e., pumping Na to Cu) causes a linear decrease in the work function. The first observation implies that at ~ −100mV the Cu surface was fully depleted of Na by electropumping. Given the linear dependence of Na XP intensities on V_{WR} above the threshold, the second observation implies that we are dealing with submonolayer coverages of Na on Cu where $\Delta\phi$ varies linearly with ϑ_{Na}.[18] Specifically, over the range of our measurements, it must be the case that $\vartheta_{Na} < 0.3$ monolayers. In fact, if we make use of the published $\Delta\phi$ data for Na/Cu(111)[19] it is straightforward to estimate the maximum value of ϑ_{Na} achieved under our conditions. This corresponds to $V_{WR} = -600$ mV, at which point the measured $\Delta\phi$ is − 0.85 eV with respect to the clean surface value. This is equivalent to $\vartheta_{Na} = 0.06$ monolayers on the basis of a pure Cu{111} surface. It should be a realistic estimate for our polycrystalline Cu sample which is composed of large particles (~5 μm) whose external surfaces will be dominated by {111} planes.

The threshold in V_{WR} for Na-induced work function decrease does not coincide with the threshold in V_{WR} for the appearance of XP detectable Na. This difference probably reflects differences in the electrode/electrolyte interface between samples. Such differences would be expected to lead to shifts in the overpotential scale (V_{WR}) but they do not affect our interpretation of the results.

The relationship between the change in the ohmic-drop free difference potential between the working and reference electrodes (ΔV_{WR}) and the change in the work function of the working electrode is a somewhat controversial subject. Vayenas et al. have derived[20] the following relationship $e\Delta V_{WR} = \Delta\phi$. They also validated it experimentally by the Kelvin probe technique[21] over certain ranges of ΔV_{WR} for both Na and oxygen ion conducting electrolytes interfaced with Pt. However Zipprich et al.[22] carried out similar measurements in which, as here, they used the secondary electron cutoff in the UP spectra to follow $\Delta\phi$. They did not find a 1:1 correlation between $e\Delta V_{WR}$ and $\Delta\phi$. As is apparent from Figure 8, neither do we. The slope of the line in Figure 9 is 2 and not unity.

The cause of these discrepancies remains unclear. It is most unlikely to be related to differences in measuring technique. With a patchy sample (as in the present case), UPS cutoff and the Kelvin probe method both provide an area-averaged value for $\Delta\phi$. Furthermore, the two methods average over similar areas of the sample surface. (In contrast with this, measurements of the photoelectric threshold provides a value for ϕ_{min}). Furthermore, in their study of the Pt/yttria-stabilized zirconia system, Metcalfe et al.[23] used the Kelvin probe method and found that the Pt electrode failed to exhibit a direct equality between change in work function and change in the ohmic-drop free potential.

For three different samples using three different experimental techniques we obtain the same results. (i) There is a range of $\Delta\phi$ values over which no Na present on the surface of the copper. (ii) After a certain threshold value of V_{WR} is exceeded, both the Na coverage and the Cu work function vary linearly with V_{WR}. However, there is no regime over which the identity $e\Delta V_{WR} = \Delta\phi$ holds. These observations are in good agreement with reactor studies of the CO+NO reaction over Pt under EP conditions.[24] These show that over a certain range of V_{WR} the catalytic rate remains at a constant (low) value. Then, beyond the threshold V_{WR} value, the rate increases strongly as V_{WR} continues to decrease. Clearly, the EP effect depends entirely on the presence of Na at the surface of the catalytically active electrode. *ϑ_{Na} is the key quantity controlling the catalytic response*. In the case of catalytic reactions involving NO reduction by CO or by propene, we have argued in detail[7,12,24] that EP is due to Na-triggered dissociation of adsorbed NO.

Why, under some conditions is ϑ_{Na} linked to V_{WR}, whereas under others, it is not?

The underlying causes for the eventual uncoupling of ϑ_{Na} and V_{WR} remain to be clarified. It seems at least possible that this behavior is connected with changes occurring at the electrode/electrolyte interface (whose properties determine the overpotential). This region is invisible to all the experimental methods that have been brought to bear thus far. All of them, including the catalytic reaction itself, are probes of the gas/solid or vacuum/solid interface. The answer to this puzzle may literally be buried. Uncovering it calls for the application of new experimental techniques.

4. Conclusions

Our work leads us to the following conclusions: (1) The coverage of electro-pumped Na on a thin film Cu catalyst contacted with a sodium ion conducting solid electrolyte is determined by the catalyst potential; the effect is fully reversible. (2) The time constants of these spill over and reverse spill over processes is short compared with 1 min. Photoelectron microscopy suggests that the spatial distribution of the Na on the Cu

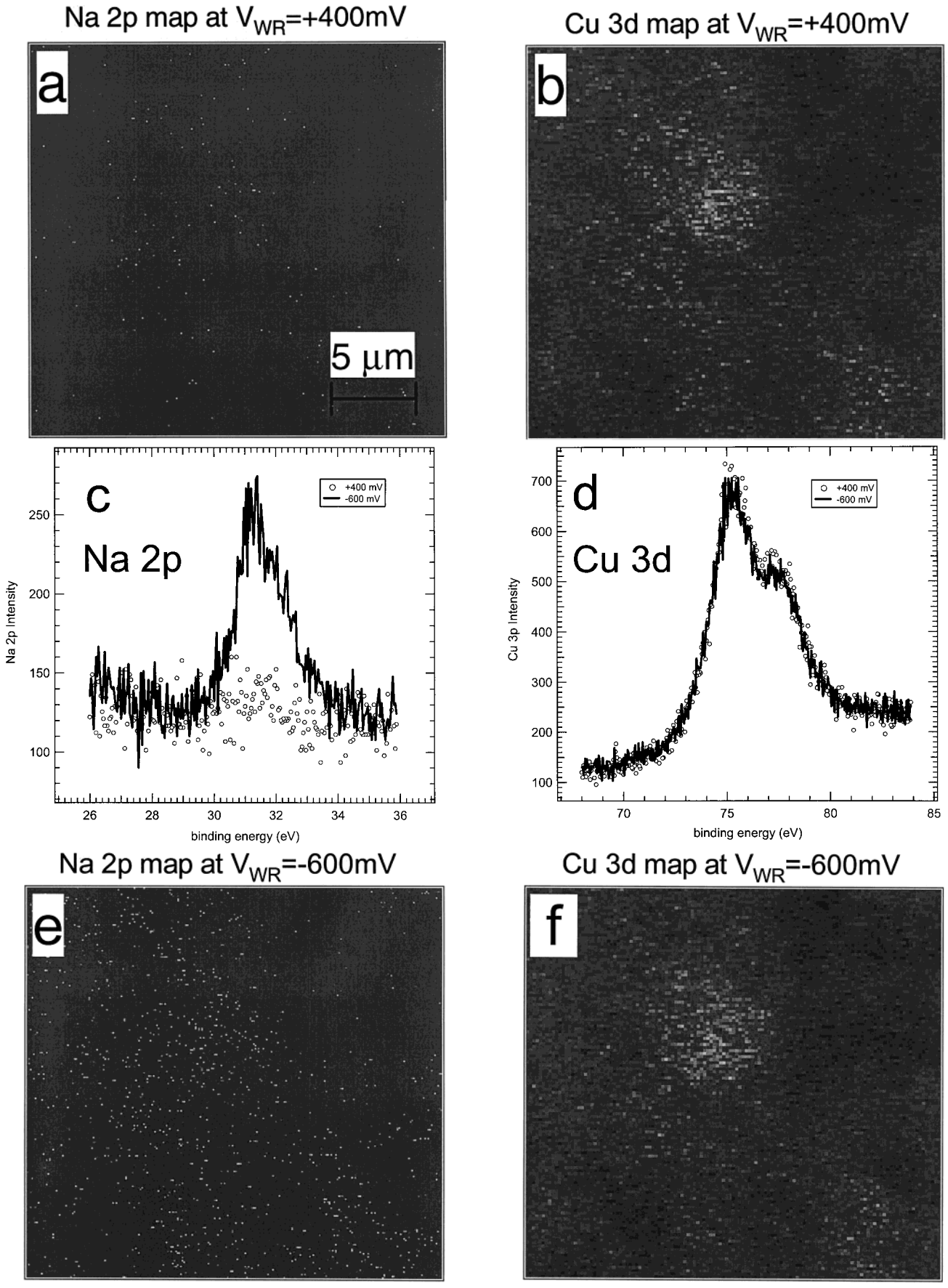

Figure 8. 25 × 25 μm^2 photoelectron intensity maps. (a) Na Na $2p_{3/2}$ at $V_{WR} = +400$ mV, (b) Cu $3d_{5/2}$ at $V_{WR} = +400$ mV, (c) and (d) XP microspot spectra taken at the center of the images, (e) Na Na $2p_{3/2}$ at $V_{WR} = -600$ mV, (f) Cu $3d_{5/2}$ at $V_{WR} = -600$ mV. All images corrected for topographic effects.

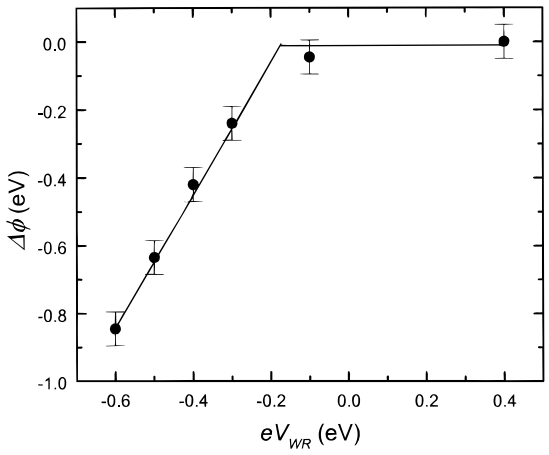

Figure 9. Work function changes of the Cu working electrode as a function of V_{WR}.

is relatively uniform. (3) Over a range of ~ 1 V, the Na coverage and Cu work function scale linearly with catalyst potential. In this regime, the Na coverage varies from zero to ~0.06 monolayer and the catalytic performance improves dramatically. (4) At sufficiently high values of catalyst potential (V_{WR}), this quantity is uncoupled from the Na coverage, work function and catalytic performance of the working electrode. (5) Electrochemical promotion of heterogeneously catalyzed reactions is due to the potential controlled effect of Na coverage on the bonding and chemistry of coadsorbed reactant species.

Acknowledgment. We thank S. Tracey, S. Gunther, L. Gregoratti, and M. Kiskinova for their invaluable assistance during the experiments at ELETTRA. F. J. Williams holds a Fundación YPF scholarship. Financial support from the U.K. Engineering and Physical Sciences Research Council and from the European Union is gratefully acknowledged under Grants GR/M76706 and BRPR-CT97-0460, respectively.

References and Notes

(1) Kiskinova, M. P. Poisoning and Promotion in Catalysis Based on Surface Science Concepts and Experiments; Elsevier: Amsterdam, 1992.
(2) Niemantsverdriet, J. W. *Appl. Phys. A* **1995**, *6*, 503.
(3) Thomson, S. J. *J. Chem. Soc., Faraday Trans.* **1987**, *83*, 2001.
(4) Ormerod, R. M.; Lambert, R. M. In *Surface Reactions* Madix, R. J., Ed., Springer Series in Surface Science, 34; Springer-Verlag; Berlin, 1994; p 89−131.
(5) Lee, A. F.; Baddeley, C. J.; Hardacre, C.; Ormerod, R. M.; Lambert, R. M.; Schmid, G.; West, H. *J. Phys. Chem.* **1995**, *99*, 6096.
(6) Bebelis, S.; Vayenas, C. G. *J. Catal.* **1989**, *118*, 125.
(7) Yentekakis, I. V.; Palermo, A.; Filkin, N. C.; Tikhov, M. S.; Lambert, R. M. *J. Phys. Chem. B* **1997**, *101*, 3759.
(8) Filkin, N. C.; Tikhov, M. S.; Palermo, A.; Lambert, R. M. *J. Phys. Chem. A* **1999**, *103*, 2680.
(9) Yentekakis, I. V.; Lambert, R. M.; Tikhov, M. S.; Konsolakis M.; Kiousis, V. *J. Catal.* **1998**, *176*, 82.
(10) Konsolakis, M.; Palermo, A.; Tikhov, M.; Lambert, R. M.; Yentekakis, Y. V. *Ionics* **1998**, *4*, 148.
(11) Konsolakis, M.; Nalbantian, L.; McLeod, N.; Yentekakis, I. V.; Lambert, R. M. *Applied Catal., B* 1999. In press.
(12) Williams, F. J.; Palermo, A.; Tikhov, M. S.; Lambert, R. M. *J. Phys. Chem.* Submitted for publication.
(13) Metcalfe, I. S. *Catalysis*, **1997**, *13*, 1.
(14) Armstrong, R. D.; Todd, M. In *Solid State Electrochemistry*; Bruce, P. G. Ed.; Cambridge University Press: Cambridge, 1995; p 277.
(15) Carley, A. F.; Roberts, M. W. *Proc. R. Soc. London A* **1978**, *363*, 403.
(16) Marsi, M.; Casalis, L.; Gregoratti, L.; Gunther, S.; Kolmakov, A.; Kovac, J.; Lonza, D.; Kiskinova, M. *J. Electron Sprectrosc. Relat. Phenom.* **1997**, *84*, 73.
(17) Gunther, S.; Kolmakov, A.; Kovac, J.; Kiskinova, M. *Ultramicroscopy* **1998**, *75*, 35.
(18) Tang, D.; McIlroy, D.; Shi, X.; Su, C.; Heskett, D. *Surf. Sci. Lett.* **1991**, *255*, L497.
(19) Shi, X.; Tang, D.; Heskett, D.; Tsuei, K. D.; Ishida, H.; Morikawa, Y. *Surf. Sci.* **1993** *290*, 69.
(20) Vayenas, C. G.; Bebelis, S.; Lintz, H. G.; *Catal. Today* **1992**, *11*, 303.
(21) Vayenas, C. G.; Bebelis, S.; Ladas, S. *Nature* **1990**, *343*, 625.
(22) Zipprich, W.; Wiemhofer, H. D.; Vohrer, U.; Gopel, W. *Ber. Bun-Senges. Phys. Chem.* **1995**, *99*, 1406.
(23) Emery, D. A.; Middleton P. H.; Metcalfe, I. S. *Surf. Sci.* **1998**, *405*, 308.
(24) Palermo, A.; Lambert, R. M.; Harkness, I. R.; Yentekakis, I. V.; Mar'ina, O.; Vayenas, C. G. *J. Catal.* **1996**, *161*, 471.